

(Preprint) AAS XX-XXX

OPTIMIZING PARKING ORBITS FOR ROUNDTRIP MARS MISSIONS

Min Qu,^{*} Raymond G. Merrill,[†] Patrick Chai[‡] and David R. Komar[§]

A roundtrip Mars mission presents many challenges to the design of a transportation system and requires a series of orbital maneuvers within Mars vicinity to capture, reorient, and then return the spacecraft back to Earth. The selection of a Mars parking orbit is crucial to the mission design; not only can the parking orbit choice drastically impact the ΔV requirements of these maneuvers but also it must be properly aligned to target desired surface or orbital destinations. This paper presents a method that can optimize the Mars parking orbits given the arrival and departure conditions from heliocentric trajectories, and it can also enforce constraints on the parking orbits to satisfy other architecture design requirements such as co-planar sub-periapsis descent to planned landing sites, due east or co-planar ascent back to the parking orbit, or low cost transfers to and from Phobos and Deimos.

INTRODUCTION

NASA's Human Spaceflight Architecture Team (HAT) is conducting a series of architecture trade studies and analyses to define the capabilities and elements needed for sending human to Mars. For any roundtrip mission to Mars, the transportation system must perform a series maneuvers within Mars vicinity to capture, reorient, and eventually escape to return back to Earth. The selection of a Mars parking orbit is crucial to the mission design and in many cases ecliptic orbits are needed for the reduced ΔV costs of going in and out of Mars' gravity well. Since the orbit tangentially captured upon arrival is typically not ideally oriented for Earth return maneuver at departure, additional reorientation maneuvers are required to not only line up the orbital plane but also the line of apside and the parking orbit of the transportation system must be chosen and optimized such that the total ΔV costs of these maneuvers are minimized. In addition, the selected parking orbit must be properly aligned to target desired surface or orbital destinations. While many previous Mars studies had over-simplified the problem and only assumed tangential arrival and departure maneuvers without taking into considerations of reorientation, several studies have addressed the reorientation techniques in the past: Landau introduced a technique called "apostwist" which makes use of orbit precessions of the arrival and departing parking orbits to line up the lines of apside and a plane change "twist" at apoapse to complete the transition.¹ He later improved the technique with off tangential burns at capture and escape maneuvers so that the overall

^{*} Staff Scientist, Analytical Mechanics Associates, Inc., 21 Enterprise Parkway, Suite 300, Hampton, Virginia 23666-6413, U.S.A.

[†] Aerospace Engineer, NASA Langley Research Center, Hampton, Virginia 23681, U.S.A. AIAA Senior Member.

[‡] Aerospace Engineer, NASA Langley Research Center, Hampton, Virginia 23681, U.S.A. AIAA Member.

^{§§} Senior Aerospace Engineer, NASA Langley Research Center, Hampton, Virginia 23681, U.S.A.

ΔV can be minimized.² Desai introduced a “free” method that optimized the inclination and semi-major axis of the parking orbit to ensure not only tangential burns at capture and escape but also a “free” transition in which no plane change or extra maneuver is required.³ The authors of this paper introduced a “bi-elliptic apotwist” technique which added additional bi-elliptic maneuvers at capture and escape in an effort to further reduce the overall ΔV costs of the reorientations maneuvers.^{4,5} This method has since evolved in the past two years and this paper details the process presently used by HAT to optimize the parking orbits while satisfying constraints imposed by different designs of the transportation systems and the mission concepts of operations.

BI-ELLIPTIC APOTWIST

The trajectory design of a roundtrip Mars mission typically starts with the optimization of the heliocentric trajectories of the transfers between Earth and Mars. Mars arrival and departure dates, along with the hyperbolic excess velocity (V_∞) vectors from the heliocentric trajectories are used as the basis for optimizing the parking orbit for the transportation vehicle. For a given incoming V_∞ vector at Mars arrival, the hyperbolic B-plane angle can uniquely determine the arriving orbital plane. Assuming a periapse altitude of 250 km, a tangential insertion burn at periapse can capture the spacecraft into a parking orbit and the magnitude of the burn is dependent on the desired size or period of the parking orbit. Similarly for a given departure V_∞ vector, the departing hyperbolic B-plane angle and magnitude of the escape burn can uniquely determine the departure parking orbit that the spacecraft must be in to complete the round trip mission. To transfer the spacecraft from the arrival parking orbit to the departure parking orbit, the traditional apotwist reorientation method solves for the B-plane angles and the time during the Mars stay such that both parking orbits precess to a point when their lines of apside coincide and a plane change maneuver at apoapse completes the transfer (with one condition that both the arrival and departure parking orbits are of the same size). The reorientation solutions from the traditional apotwist method are quite limited since only a small set of B-plane angle combinations can be found to line up the lines apside and many times they result in less desirable parking orbits and high ΔV costs. The bi-elliptic apotwist technique opens up the solution space greatly by introducing a 3-burn sequence at arrival and departure. That is, instead of directly inserting the spaceship into the arrival parking orbit, the spaceship performs a 3-burn bi-elliptic maneuver which inserts into an intermediate elliptic orbit (burn 1), followed by a plane change near apoapse (burn 2), then comes down to a second elliptic orbit before inserting into the final parking orbit (burn 3). The same bi-elliptic maneuver sequence can be used for escape but in reverse order (burns 5, 6, 7). Burn 4 is the apotwist maneuver performed at apoapse and the spaceship transitions from the arrival parking orbit to the departure parking orbit. The entire 7-burn bi-elliptic apotwist maneuver sequence is shown in Figure 1. Borrowed from the improved Landau method, the capture burn (burn1) and escape burn (burn 7) are assumed to be coplanar but non-tangential and off periapse to further open up the solution space, resulting in a greater range of parking orbit choices.

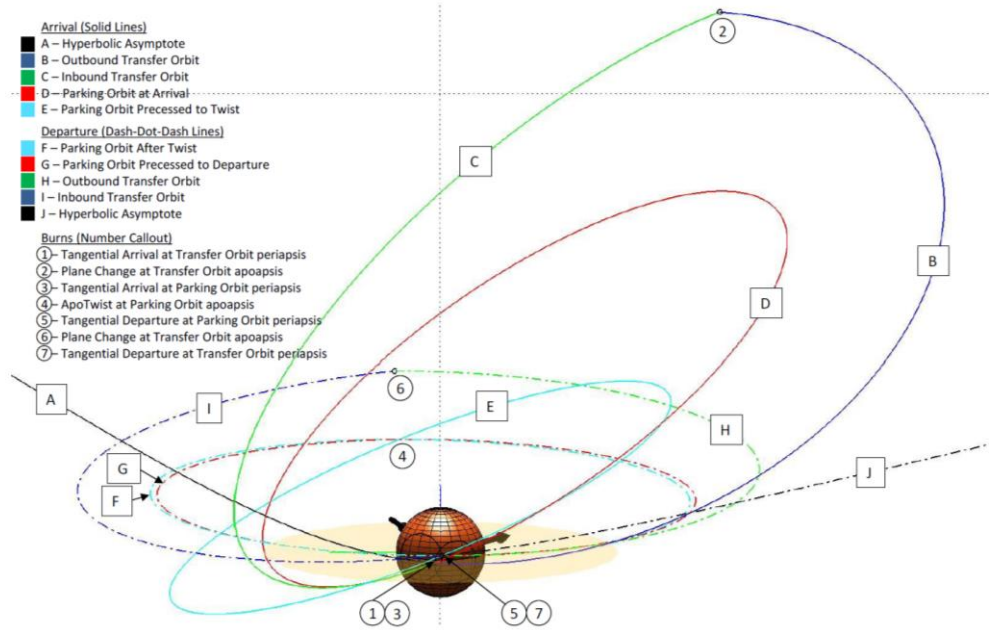


Figure 1. Bi-elliptic Apotwist Maneuver Sequence.

METHODOLOGY

The bi-elliptic apotwist reorientation can be solved by setting up a nonlinear programming problem and an off the shelf solver such as SNOPT can be used to minimize the overall ΔV cost of the 7-burn maneuver sequence. First, a set of input parameters are defined and are considered constants within the problem. They include the arrival and departure hyperbolic excess velocity vectors (\mathbf{V}_{∞}^a and \mathbf{V}_{∞}^d), Mars stay time (t_{stay}), parking orbit periapse radius (r_p) and apoapse radius (r_{a_b}) of the bi-elliptic transfer orbit. r_p is assumed to be low and equivalent of 250 km altitude to minimize the costs of capture and escape maneuvers and the deorbit burn of the lander for surface missions, while r_{a_b} is assumed to be high and equivalent of a 10-sol elliptic orbit to minimize the plane change costs for the bi-elliptic maneuvers. Second, a set of independent variables are chosen to uniquely define the arrival and departure parking orbits. Most of the independent variables are in pairs with one describing the arrival and the other describing the departure orbit. Hyperbolic B-plane angles (β^a and β^d) and radii of periapse (r_p^a and r_p^d) are independent variables used to determine the arriving and departing hyperbolic orbits. True anomalies (ta^a and ta^d) are used to define the locations (\mathbf{r}^a and \mathbf{r}^d) where capture and escape maneuvers occur to transfer from hyperbolic to the intermediate elliptic orbits. Since the capture and escape burns are assumed to be coplanar, only the radii of periapse ($r_{p_b}^a$ and $r_{p_b}^d$) of the intermediate elliptic orbits are needed as independent variables to determine the first halves of the bi-elliptic orbits. Figure 2 shows the geometry of a non-tangential, off-periapse maneuver that transitions from a hyperbolic orbit to an elliptic orbit and the line of apside of the elliptic orbit can be calculated based on the difference of true anomalies between the hyperbolic and elliptic orbit. Note $r_{p_b}^a$ and $r_{p_b}^d$ must be less than the magnitudes of \mathbf{r}^a and \mathbf{r}^d respectively and greater than r_p to ensure the orbits are well defined. To set up the bi-elliptic maneuvers at near aopapse of the intermediate elliptic orbits, true anomalies (ta_b^a and ta_b^d) are used as independent variables to define the locations (\mathbf{r}_b^a and \mathbf{r}_b^d) of the plane

change maneuvers. Rotating the orbital planes about the position vectors \mathbf{r}_b^a and \mathbf{r}_b^d with plane change angles β_b^a and β_b^d define the orbital planes of the remaining halves of the elliptic orbits. Within the rotated orbital planes, \mathbf{r}_b^a and \mathbf{r}_b^d , along with periapse radius rp and apoapse radius ra_b can uniquely define the remaining halves of the elliptic orbits, the spacecraft is assumed to perform tangential burns at periapse to transition from the bi-elliptic orbits to the final arrival and departure parking orbits with the same radius of apoapse (ra). The last independent variable is the time of the apotwist (t_{twist}) and J2 is used to calculate the orbit precession from the times of arrival and departure to t_{twist} when the lines of apside (\mathbf{a}^a and \mathbf{a}^d) of the two parking orbits are expected to line up. The orbital elements of the hyperbolic orbits, bi-elliptic orbits and parking orbits can be calculated analytically based on these independent variables, and they can be converted to position and velocity vectors at the points where maneuvers occur. The ΔV s for all seven maneuvers ($\Delta V_i, i=1, \dots, 7$) can be calculated from the velocity differences between connecting orbits and the overall problem can be summarized as follows:

Given $\mathbf{V}_\infty^a, \mathbf{V}_\infty^d, t_{stay}, rp, ra_b$, Find $[\beta^a, \beta^d, rp^a, rp^d, ta^a, ta^d, rp_b^a$ and $rp_b^d, ta_b^a, ta_b^d, ra, t_{twist}]$ that minimize the objective function

$$J = \sum_{i=1, \dots, 7} \Delta V_i$$

subject to the constraints,

$$rp < rp_b^a < |\mathbf{r}^a|$$

$$rp < rp_b^d < |\mathbf{r}^d|$$

$$\frac{\mathbf{a}^a \cdot \mathbf{a}^d}{|\mathbf{a}^a| |\mathbf{a}^d|} = 1$$

Additional constraints can be added based on specific mission requirements and are described in more details in later sections. The non-linear programming problem is solved using a gradient based optimizer and many local minimum solutions exist due to a relatively larger set of independent variables and fewer constraints. A large set of initial guesses for the independent variables can be randomly generated and the problem can be solved thousands of times to find the global optimal solution. It should also be pointed out that all variables including t_{twist} are being solved as continuous variables even though the actual apotwist can only occur once per revolution when the spacecraft reaches apoapse. This is appropriate because once the solution is found t_{twist} and the hyperbolic arrival and departure times can be re-adjusted to account for the phasing of the orbits and typically they have little to no impact on the heliocentric trajectories.

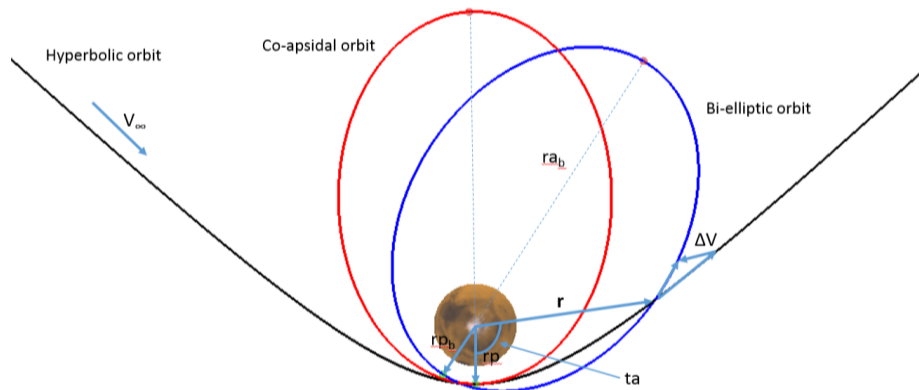


Figure 2. Co-planar non-tangential off-periapse burn at Mars arrival.

HELIOCENTRIC TRAJECTORIES

Two architecture options are being studied by HAT for crewed missions to Mars, The chemical option is the traditional impulsive approach in which chemical propulsion is used for transfers between Earth and Mars and the heliocentric trajectories are optimized by minimizing the total ΔV costs of the Trans-Mars injection, Mars orbit insertion, Trans-Earth injection and Earth orbit insertion maneuvers.^{6,7,8,9} Table 1 shows the Mars incoming and outgoing V_∞ vectors and corresponding ideal ΔV s to and from 1-sol parking orbit (assuming tangential burns at periapse) for missions between 2037 and 2045. The hybrid option is a relatively new approach that uses chemical propulsion deep in planets' gravity wells and solar electric propulsion elsewhere to create a more fuel efficient solution without significantly increase in total mission flight times. Unlike the chemical option, the heliocentric trajectories for the hybrid option are heavily dependent on the amount of acceleration the solar electric engines can generate and must be optimized individually for each architecture design choice. Table 2 shows the Mars arrival and departure conditions from the heliocentric trajectories of a particular hybrid design for missions between 2033 and 2054. The ideal capture/escape ΔV s listed for the for the hybrid option are to and from 5-sol parking orbit (as opposed to 1-sol for the chemical option) due to the design differences between the two architecture options. Figure 3 shows the ideal capture and escape ΔV to and from 1-sol, 5-sol and low Mars orbit for different incoming and outgoing V_∞ magnitudes. The ideal ΔV difference between 1-sol and 5-sol is 0.147 km/s, a significant amount for the hybrid option in which the capture/escape ΔV s are around 0.2 km/s but not much for the chemical option whose ΔV s are around 1 km/s.

Based on these Mars arrival and departure conditions, the parking orbits can be optimized using the bi-elliptic apotwist technique with additional constraints imposed for targeting orbital, surface, and missions to Phobos and Deimos. The results for these missions using both chemical and hybrid options are presented in the following sections.

Table 1. Mars arrival and departure conditions for chemical option between 2037 and 2045.

| Launch Year | Mars Arrival | V_∞ (km/s) | Decl (deg) | RA (deg) | Ideal ΔV (km/s) | Mars Departure | V_∞ (km/s) | Decl (deg) | RA (deg) | Ideal ΔV (km/s) | Stay Time (days) |
|-------------|--------------|-------------------|------------|----------|-------------------------|----------------|-------------------|------------|----------|-------------------------|------------------|
| 2037 | 8/2/2038 | 2.789 | 38.7 | 19.4 | 0.966 | 7/23/2039 | 3.097 | 8.7 | -124.1 | 1.126 | 352.8 |
| 2041 | 7/27/2042 | 2.920 | -1.7 | 113.8 | 1.033 | 7/31/2043 | 2.471 | 5.3 | -53.5 | 0.814 | 368.7 |
| 2045 | 10/6/2046 | 3.334 | -34.0 | 162.9 | 1.257 | 1/29/2048 | 2.757 | 31.6 | 34.3 | 0.950 | 480 |

Table 2. Mars arrival and departure conditions for a hybrid option between 2037 and 2054.

| Launch Year | Mars Arrival | V_∞ (km/s) | Decl (deg) | RA (deg) | Ideal ΔV (km/s) | Mars Departure | V_∞ (km/s) | Decl (deg) | RA (deg) | Ideal ΔV (km/s) | Stay Time (days) |
|-------------|--------------|-------------------|------------|----------|-------------------------|----------------|-------------------|------------|----------|-------------------------|------------------|
| 2033 | 12/30/2033 | 1.640 | 0.0 | -116.3 | 0.344 | 3/11/2035 | 1.421 | 0.0 | 127.0 | 0.278 | 435.2 |
| 2037 | 8/3/2038 | 0.949 | 13.7 | 70.9 | 0.166 | 5/30/2039 | 1.170 | -14.7 | -158.2 | 0.214 | 300 |
| 2041 | 10/5/2042 | 1.422 | -12.6 | 134.3 | 0.279 | 8/1/2043 | 1.402 | 6.4 | -91.5 | 0.273 | 300 |
| 2045 | 12/3/2046 | 1.153 | -12.4 | -151.4 | 0.210 | 9/29/2047 | 0.735 | 14.8 | -27.5 | 0.130 | 300 |
| 2050 | 2/8/2051 | 1.227 | 12.1 | -76.8 | 0.227 | 3/30/2052 | 0.999 | -13.3 | 147.0 | 0.176 | 416.1 |
| 2054 | 8/30/2055 | 1.207 | 2.5 | 101.1 | 0.223 | 6/25/2056 | 1.363 | -6.2 | -131.9 | 0.262 | 300 |

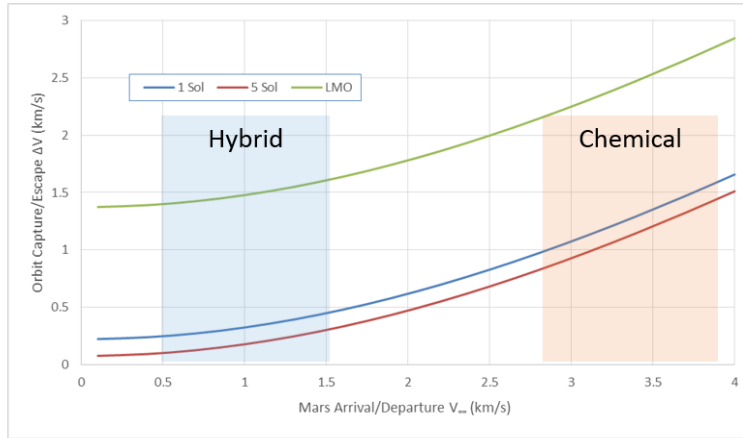


Figure 3. Ideal capture/escape ΔV for different parking orbit sizes.

ORBITAL MISSIONS

For orbital missions the spacecraft is assumed to stay in a parking orbit during the entire Mars stay and no other constraints are imposed. The periapse of the parking orbits are assumed to be of 250 km altitude, the apoapse of the bi-elliptic orbits is assumed to be equivalent of 10-sol orbit, and the period of the parking orbits is assumed to be 1-sol for the chemical option and between 1-sol to 5-sol for the hybrid option. For each mission, 2000 sets of initial guesses of the independent variables are randomly generated for the reorientation solver and typically more than half of them yield local optimal solutions. Figure 4 shows the reorientation ΔV costs versus arrival parking orbit inclination for the chemical option for launch opportunities between 2037 and 2045. Each point on the plot represents a bi-elliptic apotwist solution and the reorientation ΔV is defined as the total 7-burn maneuver ΔV minus the ideal arrival and departure ΔV s listed in table 1. The lowest cost solutions can be found with the reorientation ΔV costs around 50 m/s or less and the best solutions have retrograde parking orbits for all three missions. Prograde orbits cost around 150 m/s and polar orbits cost between 200 m/s and 300 m/s.

Figure 5 shows the reorientation costs versus arrival parking orbit inclination for the hybrid option for launch opportunities between 2033 and 2054. The color represents the parking orbit period which can be between 1-sol to 5-sol for the hybrid option and optimized by the solver while minimizing the total ΔV . The reorientation ΔV is defined as the total 7-burn maneuver ΔV minus the ideal arrival and departure ΔV s listed in table 2. While most of the solutions found reach the maximum allowable period of 5-sol, some solutions can be found to have lower periods for certain parking orbit inclinations. Most missions have the lowest reorientation costs of less than 50 m/s except for 2045 which is about 130 m/s. Prograde parking orbits are more favorable for 2037, 2041, 2045 and 2054 launch years while retrograde orbits are more favorable for 2033 and 2050.

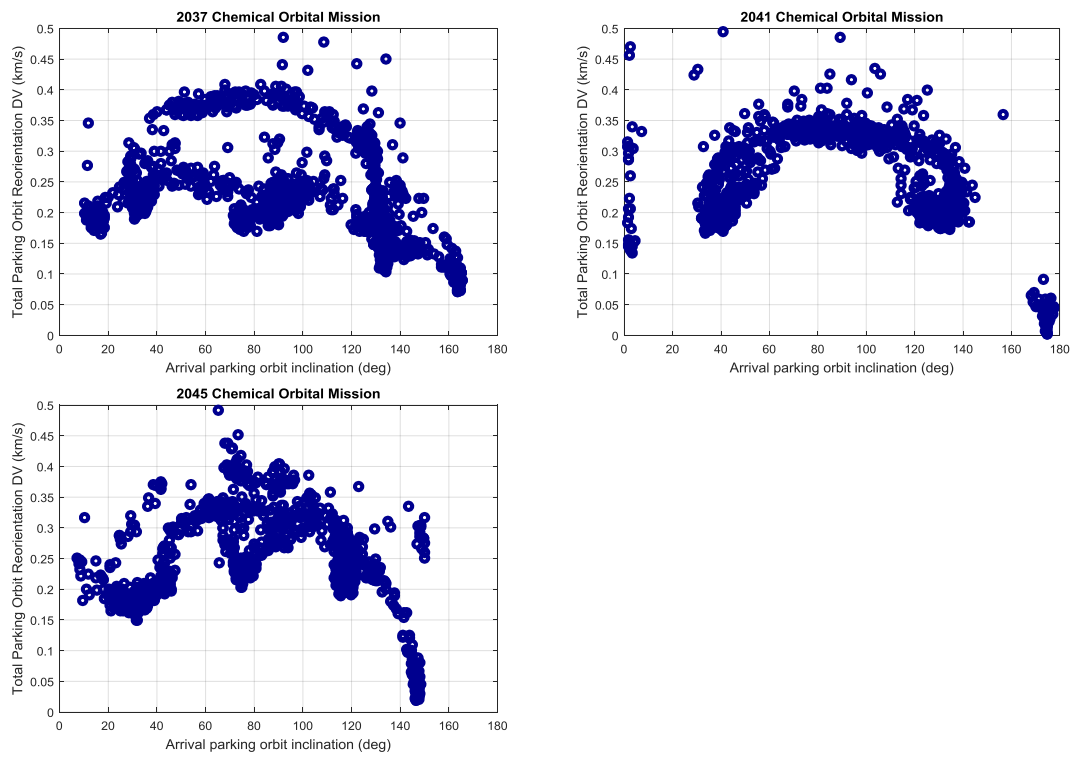


Figure 4. Orbital missions for Chemical option between 2037 and 2045.

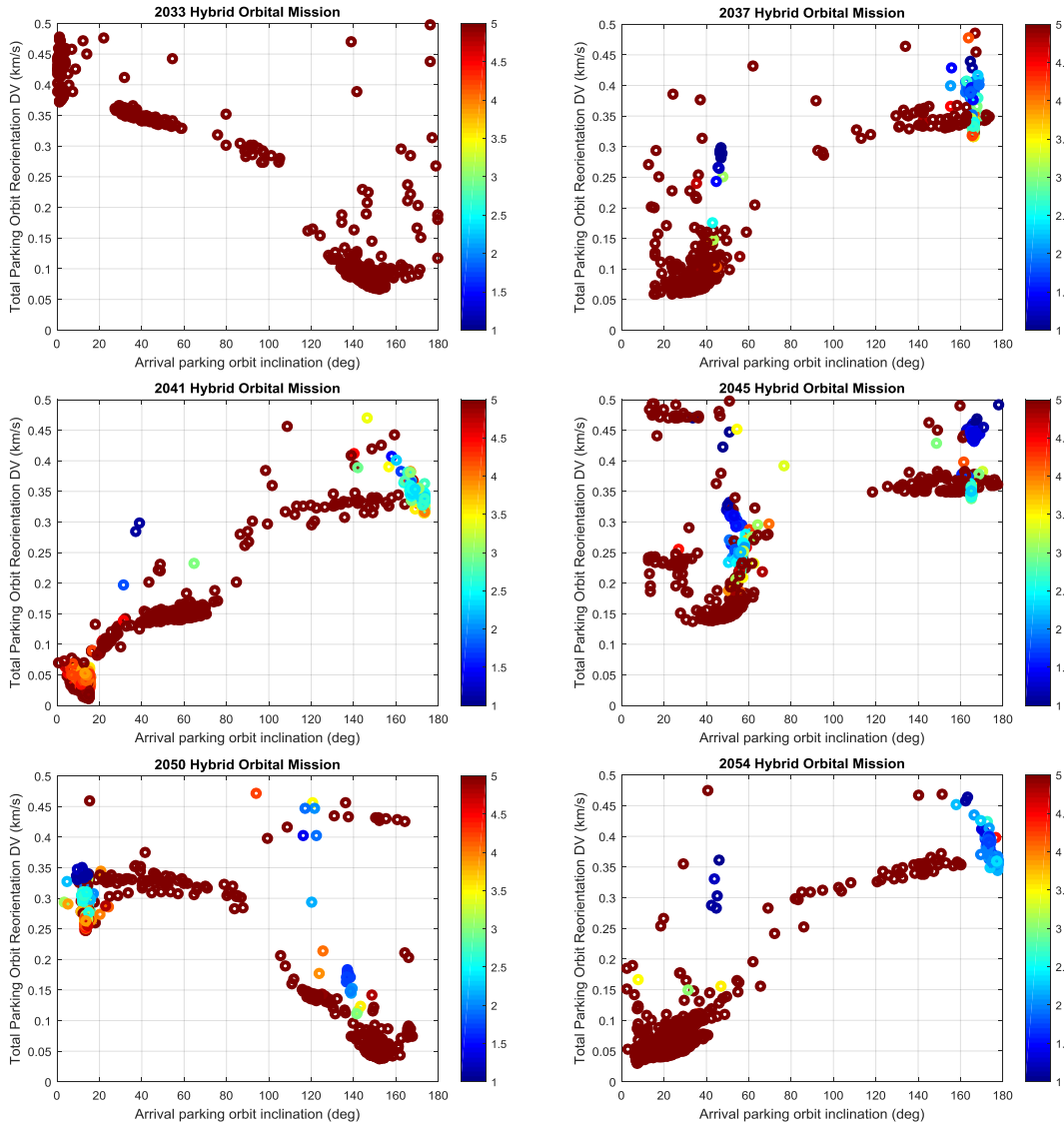


Figure 5. Orbital missions for hybrid option between 2033 and 2054.

SURFACE MISSIONS

For surface missions the transportation system is assumed to stay in parking orbits and perform the same 7-burn bi-elliptic maneuvers as the orbital missions, but with additional constraints imposed on the parking orbits. Upon Mars arrival, the spacecraft rendezvous with a lander that is already pre-deployed in the arrival parking orbit. For the current Mars architectures HAT is investigating, the design of the entry, descent and landing system requires that the landing site be directly under the parking orbit periapse such that the lander can perform a tangential deorbit burn at apoapse to transfer down towards the landing site. This translates to constraining the declination of the parking orbit periapse to be equal to the latitude of the landing site (lat), while the longitude can be aligned by the proper phasing of the spacecraft in orbit. Two types of ascent options are considered: The first option is “due-east” ascent in which the ascent stage performs due-east ascent to low Mars orbit (LMO) before making another tangential burn to rendezvous with

the transportation system which has already performed the apotwist maneuver and transitioned into the departure parking orbit. In this case a constraint must be imposed such that the inclination of the departure parking orbit is equal to the latitude of the landing site. The second option is “taxi” ascent in which the ascent stage performs a due-east or co-planar ascent to LMO and rendezvous with a taxi vehicle that is pre-deployed and then the taxi transfers from LMO to the departure parking orbit. In this case no additional constraint is needed for the departure parking orbit and the taxi is assumed to have enough ΔV capability to transfer from LMO to the elliptic parking orbit between 1-sol and 5-sol. Like the orbital case, 2000 sets of initial guesses of the independent variables are randomly generated for the solver and the reorientation ΔV is defined as the total 7-burn maneuver ΔV minus the ideal capture and escape ΔV s for each mission.

Figure 6 shows the best reorientation solutions found for the chemical option targeting different landing site latitudes, and Figure 7 shows the results for the hybrid option. One of the most important questions regarding surface missions to understand the costs of accessing the same landing site across all launch opportunities, and it can be seen that the reorientation costs can become expensive when landing site latitude goes beyond ± 30 degrees. Table 3 shows the best reorientation solutions found targeting Jezero Crater (18.8 degrees latitude) for the due-east option across all opportunities. Since the departure parking orbit inclination matches the landing site latitude, the ascent stage only needs to perform an apoapse raise maneuver at LMO to reach the parking orbit and the ΔV s for that maneuver are listed in the last column. Note that the 2050 hybrid case has an optimal parking orbit period of 3.3 sol, therefore a lower ΔV cost for that maneuver. Some of the hybrid opportunities such as 2033 maybe difficult due to the fact that the reorientation cost accounts for a significant amount of its overall chemical ΔV budget. Table 4 shows the best reorientation solutions found for the taxi option. In this case the departure parking orbit is not aligned with the landing site (in some cases the parking orbits are retrograde) and the ascent stage can either perform a due-east ascent to a LMO with an inclination of 18.8 degrees, or a coplanar ascent to a LMO with an inclination between 18.8 and 161.2 degrees. The coplanar ascent is more costly for the ascent stage, but it may help dramatically reduce the ΔV cost for the taxi transferring from LMO to the parking orbit, as shown in all the chemical cases and the 2050 hybrid case. It should be noted that the results shown in Tables 3 and 4 represent the two extremes with the due-east option most favorable to the ascent stage and taxi option most favorable to the transportation system. Other solutions that find the balance between ascent stage, taxi and transportation are also available (but not shown) and may be more desirable for specific missions.

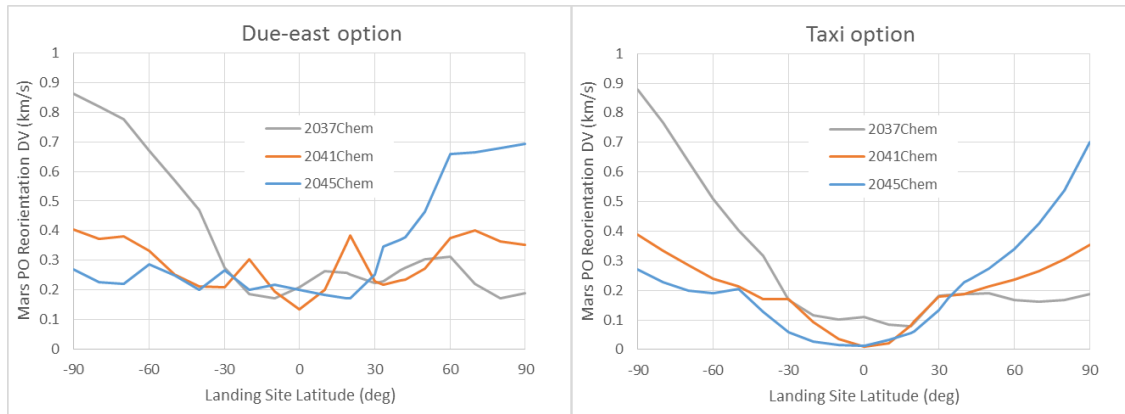


Figure 6. Surface missions for the chemical option between 2037 and 2045

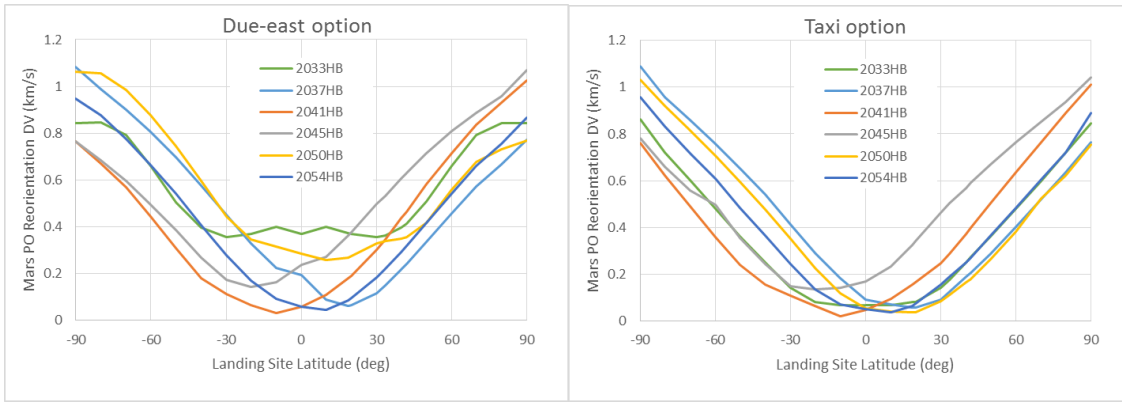


Figure 7. Surface missions for the hybrid option between 2033 and 2054.

Table 3. Due East option for surface missions to Jezero crater.

| Case | Arrival PO Inclination (deg) | Arrival PO AOP (deg) | Departure PO Inclination (deg) | Departure PO AOP (deg) | PO Period (sol) | Total ΔV (km/s) | Reorientation ΔV (km/s) | ΔV LMO to departure PO (km/s) |
|------------|------------------------------|----------------------|--------------------------------|------------------------|-----------------|-------------------------|---------------------------------|---------------------------------------|
| 2037Chem | 20.2 | -249.2 | 18.8 | -93.5 | 1.0 | 2.350 | 0.258 | 1.199 |
| 2041Chem | 18.8 | -272.6 | 18.8 | -109.4 | 1.0 | 2.206 | 0.359 | 1.199 |
| 2045Chem | 19.1 | -260.2 | 18.8 | -45.2 | 1.0 | 2.381 | 0.173 | 1.199 |
| 2033Hybrid | 19.0 | -277.9 | 18.8 | -244.7 | 5.0 | 0.995 | 0.372 | 1.345 |
| 2037Hybrid | 20.4 | -247.9 | 18.8 | -230.2 | 5.0 | 0.441 | 0.061 | 1.345 |
| 2041Hybrid | 32.4 | -217.0 | 18.8 | -214.7 | 5.0 | 0.731 | 0.179 | 1.345 |
| 2045Hybrid | 36.3 | -212.9 | 18.8 | -214.8 | 5.0 | 0.703 | 0.364 | 1.345 |
| 2050Hybrid | 19.6 | -254.0 | 18.8 | -204.4 | 3.3 | 0.673 | 0.269 | 1.320 |
| 2054Hybrid | 33.5 | -215.7 | 18.8 | -214.6 | 5.0 | 0.570 | 0.085 | 1.345 |

Table 4. Taxi option for surface missions to Jezero crater.

| Case | Arrival PO Inc (deg) | Arrival PO AOP (deg) | Departure PO Incl (deg) | Departure PO AOP (deg) | PO Period (sol) | Total ΔV (km/s) | Reorient ΔV (km/s) | ΔV LMO To departure PO (km/s) | Co-planar Ascent LMO Incl (deg) | Co-planar Ascent taxi ΔV (km/s) |
|------------|----------------------|----------------------|-------------------------|------------------------|-----------------|-------------------------|----------------------------|---------------------------------------|---------------------------------|---|
| 2037Chem | 161.1 | -265.1 | 161.1 | -109.5 | 1 | 2.171 | 0.079 | 2.096 | 161.1 | 1.198 |
| 2041Chem | 161.1 | -274.2 | 161.1 | -111.1 | 1 | 1.928 | 0.081 | 2.095 | 161.1 | 1.199 |
| 2045Chem | 145.2 | -214.4 | 145.2 | -67.5 | 1 | 2.263 | 0.055 | 2.589 | 145.2 | 1.199 |
| 2033Hybrid | 147.0 | -216.3 | 147.0 | -191.5 | 5 | 0.703 | 0.080 | 1.617 | 18.8 | 1.617 |
| 2037Hybrid | 20.4 | -247.9 | 20.4 | -225.3 | 5 | 0.438 | 0.058 | 1.350 | 19.9 | 1.346 |
| 2041Hybrid | 40.7 | -209.6 | 40.7 | -197.2 | 5 | 0.706 | 0.155 | 1.406 | 40.7 | 1.345 |
| 2045Hybrid | 44.2 | -207.5 | 44.2 | -197.1 | 5 | 0.666 | 0.326 | 1.416 | 44.2 | 1.345 |
| 2050Hybrid | 152.2 | -223.7 | 152.2 | -196.3 | 5 | 0.442 | 0.038 | 1.623 | 152.2 | 1.345 |
| 2054Hybrid | 37.2 | -212.2 | 37.1 | -197.8 | 5 | 0.550 | 0.065 | 1.396 | 25.3 | 1.377 |

MISSIONS TO PHOBOS AND DEIMOS

The Phobos/Deimos missions are essentially orbital missions, except that upon arrival the transportation system rendezvous with a taxi that is pre-deployed in the arrival parking orbit. The taxi then transfers to Phobos or Deimos, and depending on the duration of the mission it can either return to the arrival parking orbit or the departure parking orbit. The transfer between Phobos/Deimos and the parking orbit is a 2-burn maneuver shown in Figure 8, and the ΔV cost depends on the inclination and argument of periaapse of the parking orbit. Figures 9 and 10 show the ΔV costs of the taxi for each reorientation solution found for the orbital missions. The y-axis is the roundtrip ΔV to go from the arrival parking orbit to Phobos and then return to the departure parking orbit, and the colors represent the roundtrip ΔV to Deimos. Some of the ΔV s are very high due to the fact that many of the solutions found have retrograde parking orbits. Retrograde parking orbits should be avoided for Phobos/Deimos missions and those solutions can be filtered out based on the ΔV capability of the taxi vehicle.

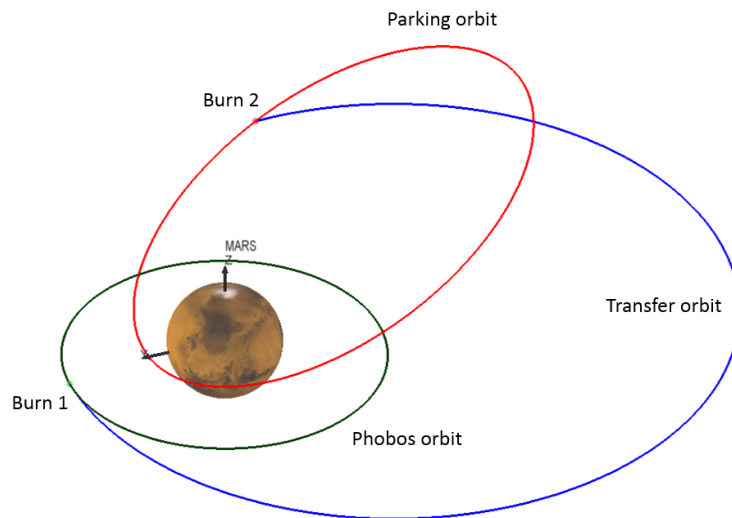


Figure 8. Trajectory from Phobos to a 1-sol parking orbit.

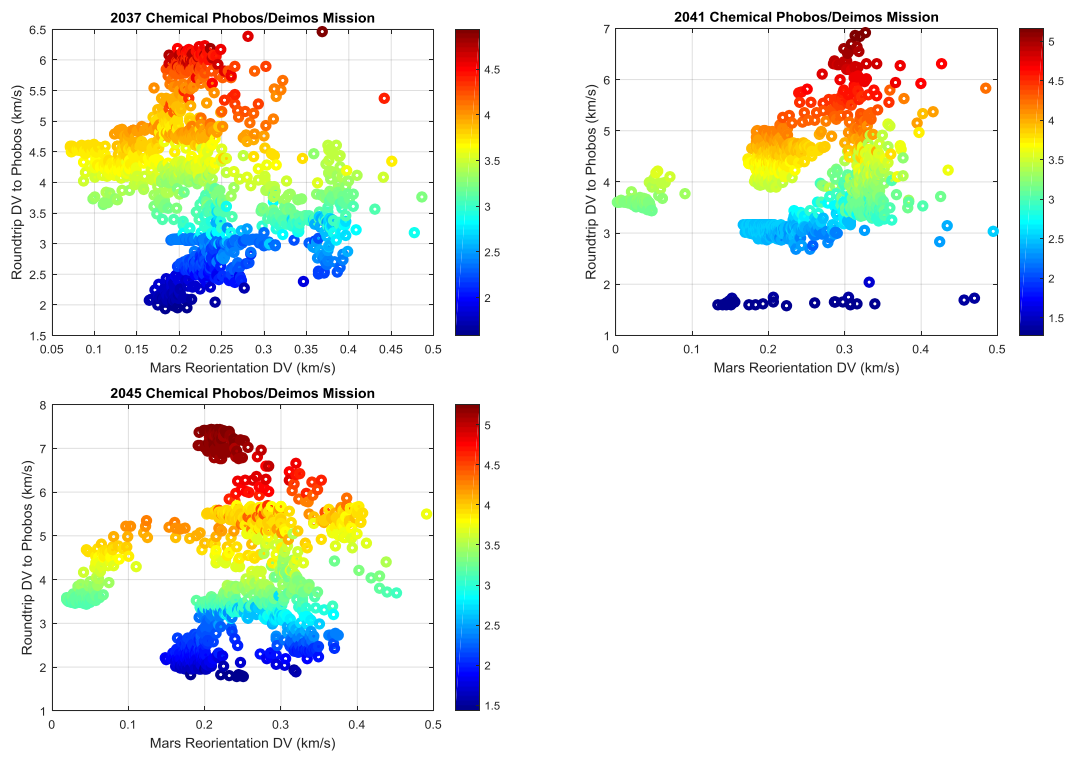


Figure 9. Missions to Phobos and Deimos for the chemical option.

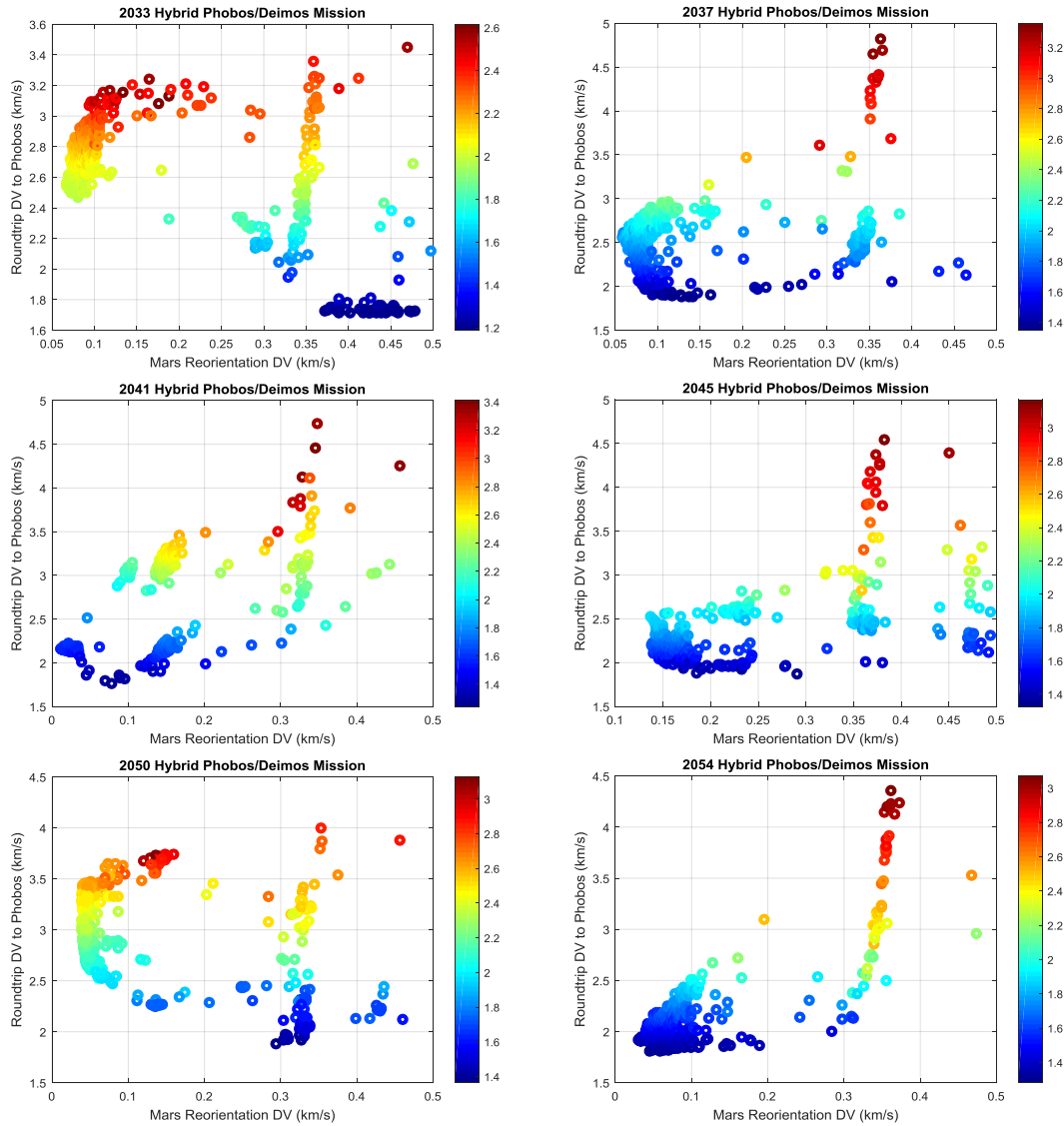


Figure 10. Missions to Phobos and Deimos for the hybrid option.

CONCLUSION

A maneuver sequence (up to seven burns), called bi-elliptic apotwist, is used and must be performed by the Mars transportation system to capture itself into a parking orbit, reorient sometime later in the mission, and then escape Mars sphere of influence to complete the roundtrip mission. The degrees of freedom introduced by the bi-elliptic maneuver sequence are large enough that parking orbits of different periods, inclinations and eccentricities can be found to satisfy both the arrival and departure conditions. Additional constraints can be imposed on the parking orbits to meet the design requirements of the system architecture such as co-planar sub-periapsis descent, due east ascent or coplanar ascent. The entire sequence can be solved as a nonlinear programming problem with an objective of minimizing the total ΔV of the seven maneuvers. Results for orbital, surface, and Phobos/Deimos missions using both chemical and hybrid architecture options are presented. A few missions from launch opportunities between 2033 and 2054 favor retrograde

parking orbits, which may be feasible for orbital missions, but may present challenges for the ascent and taxi stages in surface and Phobos/Deimos missions. To address these challenges, the ongoing studies at HAT are looking at expanding the boundary conditions beyond Mars to include heliocentric trajectories as part of the optimization process in an effort to find globally optimized solutions.

REFERENCES

- ¹ D. Landau, J. Longuski, and P. Penzo, "Method for Parking Orbit Reorientation for Human Missions to Mars," *Journal of Spacecraft and Rockets*, Vol. 42, No. 3, pp. 517–522, 2005.
- ² D. Landau, "Orbital Transfer Techniques for Round-Trip Mars Missions," Paper AAS13-449, AAS/AIAA Spaceflight Mechanics Meeting, Kauai, Hawaii, 2013.
- ³ P. Desai, J. Buglia, "Determining Mars Parking Orbits that Ensure Tangential Periapsis Burns at Arrival and Departure", *Journal Of Spacecraft And Rockets*, Vol. 30, No. 4, July-August 1993.
- ⁴ M. Qu, R.G. Merrill, P. Chai, and D.R. Komar, "Trajectory Designs for a Mars Hybrid Transportation Architecture," AAS Paper 15-522, 2015 AAS/AIAA Astrodynamics Specialist Conference, Vail, CO, August 2015.
- ⁵ R.G. Merrill, D.R. Komar, P. Chai, and M. Qu, "Optimizing Mars Sphere of Influence Maneuvers for NASA's Evolvable Mars Campaign," 2016 AIAA Space Conference, September 2016.
- ⁶ R. Merrill, N. Strange, M. Qu, and N. Hatten, "Mars Conjunction Crewed Missions with a Reusable Hybrid Architecture", paper IEEE 978-1-4799-5379-0, IEEE Aerospace Conference, 2015.
- ⁷ T. Percy, M. McGuire, and T. Polsgrove, "In-space Transportation for NASA's Evolvable Mars Campaign," 2015 AIAA SPACE Conference, Pasadena, CA, 2015.
- ⁸ R.G. Merrill, P. Chai, and M. Qu, "An Integrated Hybrid Transportation Architecture for Human Mars Expeditions," 2015 AIAA SPACE Conference, Pasadena, CA, 2015, AIAA 2015-4442.
- ⁹ P. Chai, R.G. Merrill, and M. Qu, "Mars Hybrid Propulsion System Trajectory Analysis Part I: Crew Missions," 2015 AIAA SPACE Conference, Pasadena, CA, 2015.